PACS numbers: 42.55.Rz; 42.60.Da
DOI: 10.1070/QE2007v037n06ABEH013425

Analysis of the pump-beam path in a corner-pumped slab laser

Chen Li, Qiang Liu, Mali Gong, Gang Chen, Ping Yan

Abstract. **The propagation of the pump radiation in active slab elements is considered. Conditions of the total internal reflection of the pump radiation are obtained, and are used to construct a series of graphical illustrations of reflection characteristics of different active elements.**

Keywords: *slab laser, pump, total internal reflection.*

1. Introduction

There exist several typical geometries to pump solid-state slab lasers such as face-pumping [1], edge-pumping [2], end-pumping [3], and corner-pumping [4 – 8]. The face-pumping geometry is not quite suitable for quasi-three-level media because in this geometry the pump radiation is absorbed in the direction of slab thickness. In this case, due to the relatively low absorption coefficient of the material, the pump is inefficient. However, because of a much longer pump absorption length, the remaining three pump methods are more efficient, which was confirmed experimentally. The kilowatt cw output power was obtained in the most commonly used Yb : YAG quasi-three-level material [2 – 8].

The previous experimental results [4 – 8] showed that corner-pumping geometry is a reliable and efficient way to generate pumping in quasi-three-level media. In this case, corners of the laser slab are used to couple radiation, instead of ends or edges. Pump radiation is directed to the corner surfaces by the focusing element and is confined inside the slab by total internal reflections (TIRs), resulting in multiple absorptions and therefore high absorption efficiency and uniform pump power distribution. The most important advantage of the corner-pumped geometry is that it provides a longer absorption length than other geometries due to multiple reflections inside the slab. Therefore, a question arises as to what the requirements to pump beam and laser material should be satisfied to ensure the TIR. Answering this question is significant as it will allow one to select properly the parameters of the pump radiation and the laser material to enhance the pump absorption efficiency. In this paper, we determine conditions under which the pump radiation is confined inside the slab and analyse the obtained relations.

Chen Li, Qiang Liu, Mali Gong, Gang Chen, Ping Yan Center for Photonics and Electronics, State Key Laboratory of Tribology, Department of Precision Instruments, Tsinghua University, Beijing 100084, P.R. China; e-mail: c.li@mail.tsinghua.edu.cn

Received 13 September 2006; revision received 30 October 2006
Kvantovaya Elektronika **37** (6) 541 – 544 (2007)
Submitted in English

2. A simplified model of a rectangular slab

Consider for simplicity the propagation of pump radiation in a simple rectangular slab. Figure 1 shows that the pump radiation goes into the slab through side surface 1 and then after refraction, is reflected at surface 2 perpendicular to surface 1. Let us denote the refraction angle from surface 1 by θ_1 and the incident angle from surface 2 by θ_2. It is obvious that,

$$\theta_1 + \theta_2 = 90°. \quad (1)$$

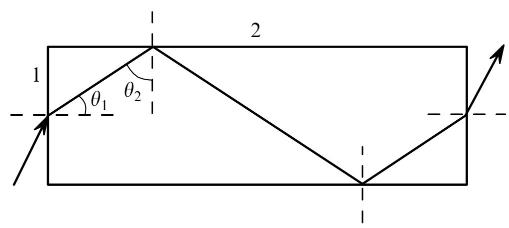

Figure 1. Pump radiation reflection in a rectangular slab.

Therefore, the laser materials are divided into two categories by the refraction index for respective discussion. In the material with refraction index equal to or greater than $\sqrt{2}$, the critical angle θ_c is equal to or less than 45°, so we obtain

$$\theta_2 = 90° - \theta_1 > 90° - \theta_c \geqslant \theta_c. \quad (2)$$

In this case, it means that once the pump beam enters the slab at one surface, it can not exit the slab until it reaches the opposite surface.

The second category represents materials with refraction index less than $\sqrt{2}$. For these materials, the critical angle θ_c is greater than 45°. Therefore, the pump beam with a larger angle of incidence at surface 1 may not satisfy the TIR condition at surface 2 and thus exit the slab. However, for the majority of popular matrixes such as YAG, YLF, and

YVO_4, the refraction indices are greater than $\sqrt{2}$ [9], and hence, the absorption length during the propagation of pump radiation inside the active element can be equal to the slab length (end-pumping) or to the slab width (edge-pumping).

3. Analyses of the corner-pumped slab

The slabs used in practice differ from the simplified rectangular slabs by the presence of four facets to couple in pump radiation. An example of such an element is presented in Fig. 2 in which only one facet is plotted for simplicity. In this case, the beam path inside the element is more complicated. Depending on the relationship between facet angle θ_0 and critical angle θ_c, this problem can be divided into four cases. In the expression below, the angle of incidence counted counterclockwise from the normal to the facet plane is denoted by θ^+ (Fig. 2a, c), and the angle of incidence counted clockwise from the normal is denoted by θ^- (Fig. 2b, d); n is the refraction index of the material. For clearness, we considered the critical case when the incidence angle of the pump beam at surface 1 or 2 is equal to the critical angle θ_c.

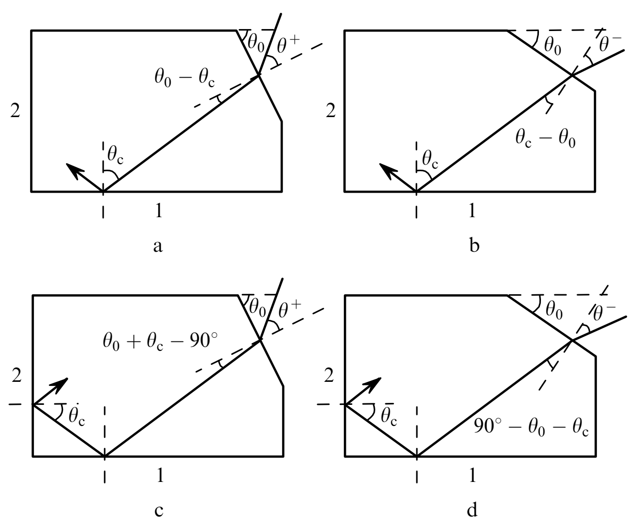

Figure 2. Pump beam reflections inside the corner-pumped slab.

3.1 Reflection from surface 1

If $\theta_0 \geqslant \theta_c$, then we obtain from Fig. 2a

$$\theta^+ = \arcsin[n\sin(\theta_0 - \theta_c)]. \tag{3}$$

Therefore, the TIR condition for the pump beam incident on surface 1 has the form

$$\begin{aligned} &0 \leqslant \theta^+ \leqslant \arcsin[n\sin(\theta_0 - \theta_c)], \\ &0 \leqslant \theta^- \leqslant 90°. \end{aligned} \tag{4}$$

If $\theta_0 < \theta_c$, then we obtain from Fig. 2b

$$\theta^- = \arcsin[n\sin(\theta_c - \theta_0)], \tag{5}$$

and the TIR condition has the form

$$\begin{aligned} &\theta^+ \in \Phi, \\ &\arcsin[n\sin(\theta_c - \theta_0)] \leqslant \theta^- \leqslant 90°. \end{aligned} \tag{6}$$

Hereafter, Φ is an empty set or null set.

3.2 Reflection from surface 2

If $\theta_0 + \theta_c \geqslant 90°$, then we obtain from Fig. 2c

$$\theta^+ = \arcsin[n\sin(\theta_0 + \theta_c - 90°)]. \tag{7}$$

Therefore, the TIR condition has the form

$$\begin{aligned} &\arcsin[n\sin(\theta_0 + \theta_c - 90°)] \leqslant \theta^+ \leqslant 90°, \\ &\theta^- \in \Phi. \end{aligned} \tag{8}$$

If $\theta_0 + \theta_c < 90°$, then we obtain from Fig. 2d

$$\theta^- = \arcsin[n\sin(\theta_c - \theta_0)], \tag{9}$$

and the TIR condition has the form

$$\begin{aligned} &0 \leqslant \theta^+ \leqslant 90°, \\ &0 \leqslant \theta^- \leqslant \arcsin[n\cos(\theta_0 + \theta_c)]. \end{aligned} \tag{10}$$

Analysis of all the above cases gives the range of incidence angles within which the pump beam will be totally reflected from both surfaces 1 and 2. By generalising the above, we can write the following.

(i) When $\theta_0 \geqslant \theta_c$ and $\theta_0 + \theta_c \geqslant 90°$,

$$\begin{aligned} &\arcsin[n\sin(\theta_0 + \theta_c - 90°)] \leqslant \theta^+ \leqslant \arcsin[n\sin(\theta_0 - \theta_c)], \\ &\theta^- \in \Phi. \end{aligned} \tag{11}$$

(ii) When $\theta_0 \geqslant \theta_c$ и $\theta_0 + \theta_c < 90°$,

$$\begin{aligned} &0 \leqslant \theta^+ \leqslant \arcsin[n\sin(\theta_0 - \theta_c)], \\ &0 \leqslant \theta^- \leqslant \arcsin[n\cos(\theta_0 + \theta_c)]. \end{aligned} \tag{12}$$

(iii) When $\theta_0 < \theta_c$ and $\theta_0 + \theta_c \geqslant 90°$,

$$\theta^+ \in \Phi, \quad \theta^- \in \Phi. \tag{13}$$

(iv) When $\theta_0 < \theta_c$ and $\theta_0 + \theta_c < 90°$,

$$\begin{aligned} &\theta^+ \in \Phi, \\ &\arcsin[n\sin(\theta_c - \theta_0)] \leqslant \theta^- \leqslant \arcsin[n\cos(\theta_0 + \theta_c)]. \end{aligned} \tag{14}$$

Note that upon total internal reflection of the pump beam surfaces 1 and 2, this condition is valid for other facets of the slab. Therefore, if the beam is incident on one of the facets at an angle satisfying conditions (11), (12), (14), it will be confined inside the slab until it reaches other facets. In this case, we neglect the possible non-parallelism of opposite facets caused by the manufacturing error or peculiarities of the profile in the case of noise suppression [2]. Thus, to reduce possible losses of the pump radiation, the slab corner facet should be small.

Recall again that depending on the value of the refraction index, we divide the laser materials into two categories: one is $n \geqslant \sqrt{2}$ and $\theta_c \leqslant 45°$ the other is $n < \sqrt{2}$ and $\theta_c > 45°$.

For the first category, above expressions (11) (12) and (14) can be simplified.

(i) When $\theta_0 \geqslant 90° - \theta_c$,

$$\arcsin[n\sin(\theta_0 + \theta_c - 90°)] \leqslant \theta^+ \leqslant \arcsin[n\sin(\theta_0 - \theta_c)], \quad \theta^- \in \Phi. \tag{15}$$

(ii) When $\theta_c \leqslant \theta_0 < 90° - \theta_c$,

$$0 \leqslant \theta^+ \leqslant \arcsin[n\sin(\theta_0 - \theta_c)], \quad 0 \leqslant \theta^- \leqslant \arcsin[n\cos(\theta_0 + \theta_c)]. \tag{16}$$

(iii) When $\theta_0 < \theta_c$,

$$\theta^+ \in \Phi, \quad \arcsin[n\sin(\theta_c - \theta_0)] \leqslant \theta^- \leqslant \arcsin[n\cos(\theta_0 + \theta_c)]. \tag{17}$$

The simple analysis shows that for the second category there exist no angles of incidence for which the pump beam experiences TIRs simultaneously from surfaces 1 and 2.

It is obvious from expression (16) that for $\theta_0 = 45°$, angles θ^+ and θ^- have equal limiting values for the TIR. Figure 3 shows the dependence of the maximum of θ^+ and θ^- on the refraction index n for $\theta_0 = 45°$ and $n \geqslant \sqrt{2}$. First, this dependence is nearly linear and gradually becomes steeper with increasing the refraction index. In the case $n > 2.613$, the maximum of θ^+ and θ^- reaches 90°, which means that at any angle of incidence, the pump radiation will be totally reflected inside the slab and thus will have no chance to escape. If the facets are present, the pump radiation can exit the slab through them. Figure 3 also shows that to increase the pump absorption efficiency in the corner-pumped geometry, the slab material should have large refraction indices. Therefore, YAG and YVO_4 matrixes are better than YLF.

Consider the Yb : YAG active element as an example. Because the refraction index of Yb : YAG is approximately 1.82, the critical angle for this material is $\theta_c = 33.3°$. Figure 4 shows the range of incidence angles calculated for different facet angles θ_0 within which the pump radiation will be totally reflected from both surface 1 and 2. To make more pump beams satisfy the TIR condition, the facet angle θ_0 should be chosen from the range $33.3° \leqslant \theta_0 \leqslant 56.7°$. When θ_0 changes from 33.3° to 56.7°, the maximum of θ^+ varies from 0 to 46.3°, while the maximum of θ^- varies from 46.3° to 0. When $\theta_0 = 45°$, the maxima of θ^+ and θ^- are both equal to 21.7°.

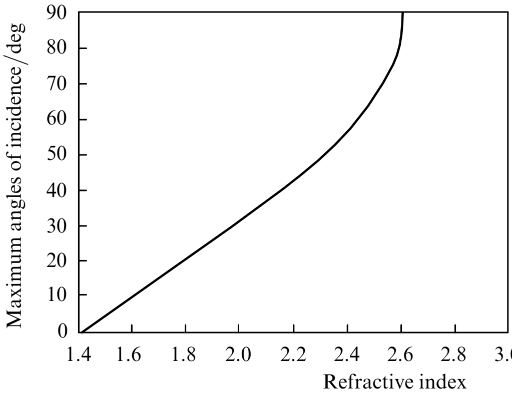

Figure 3. The dependence of the maxima of θ^+ and θ^- on the refraction index.

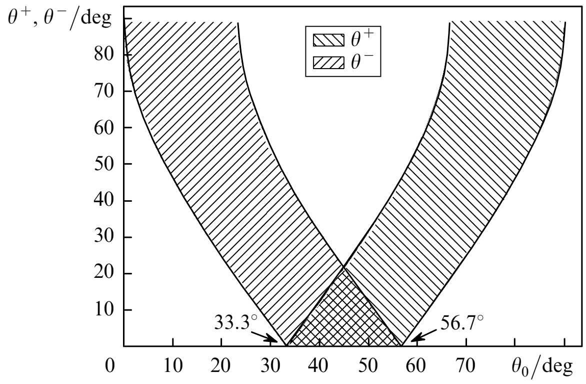

Figure 4. The range of admissible incidence angles θ^+ and θ^- as a function of the facet angle θ_0; $n = 1.82$.

In practice, the pump radiation is usually coupled to the laser slab by focusing element, such as a fiber bundle [2] or lens duct [3–6]. By using these two coupling methods, the pump power distribution is typically stronger at the center and weaker at both sides. In this case, the facet angle θ_0 should be chosen 45° to confine more pump power inside the slab. Furthermore, if we take into account the exponential law of the pump power absorption, then according to (4), it is obvious that the angle θ_0 should be slightly larger than 45°. Under this condition, more pump radiation can be totally reflected at surface 1 and therefore the slab absorbs more pump power.

We have discussed the pump radiation reflection at side surfaces of the laser slab. Now consider in more detail the reflection from the facet surfaces. It follows from the above analysis that in a corner-pumped slab, the angle between the side surface and facet plane should be as close to 45° as possible. After several reflections from side surfaces and absorption by the laser active ions, the attenuated pump radiation may finally reach facet plane at an angle close to 90°. In this case the Fresnel losses at the facet plane are present, but they are not significant. If the required profile of the slab and the design of the focusing optics are used, it is possible to decrease the area of the facet cut and correspondingly the above losses.

4. Experimental results

Our group has published a series of experimental results obtained from a corner-pumped Yb : YAG/YAG composite slab laser [4–8]. This slab is diffusion-bonded from a Yb : YAG slab of 1 mm in thickness, 4 mm in width, and 42 mm in length together with two undoped YAG slabs with original dimensions of 1 mm × 2 mm × 42 mm. Three slabs are sandwiched together from their 1 mm × 42 mm surfaces (Fig. 5). After splicing, the composite slab is cut at four corners to form facets of 1 mm × 2.8 mm, through which pump radiation is coupled. According to the theoretical analysis proposed above, our composite slab is cut along 45° for efficient pump absorption and manufacture convenience. The corner-pumped laser using this composite slab emits up to 1050 W with the slope efficiency of 42.8 % and light-to-light efficiency of 33.6 % [8]. This fairly good efficiency indicates that pump power is well absorbed inside the composite slab.

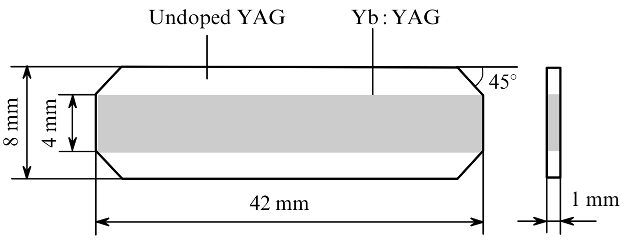

Figure 5. A composite Yb : YAG/YAG slab with 45° facets [4–8].

Ray-tracing calculations for various facet angles θ_0 have been performed. The calculated pump absorption efficiency is presented in Table 1. One can see from Table 1 that composite slab with the facet angle $\theta_0 = 50°$ exhibits the maximum absorption efficiency, which agrees well with the analysis in section 3.

Works are being performed at present to further increase the pump efficiency. Despite great technological complexity, composite slabs with various facet angles slightly larger than 45° are being manufactured. In the near future, we plan to test and compare their lasing characteristics.

Table 1. The pump absorption efficiency by a composite slab (Fig. 5) for different facet angles 45° (the concentration of activators in the Yb : YAG element is 0.5 at. %, and the pump wavelength is 940 nm).

θ_0/deg	η_{abs} (%)
45	81.38
50	86.69
55	86.02

5. Conclusions

The propagation of the pump beam in a corner-pumped slab has been studied. Conditions under which the pump beam can be totally reflected inside the slab are deduced. The obtained relations are of great interest for increasing the pump absorption efficiency in slab lasers. A laser slab made of the material with refraction index less than $\sqrt{2}$ can not confine the pump radiation inside. If the refraction index is equal to or greater than $\sqrt{2}$, there exists a range of incidence angle within which pump radiation will be totally reflected at all the inner surfaces of the slab and thus be confined inside it. It has been also shown that the slab facet angle should be close to 45° to enhance the pump absorption efficiency.

References

1. Martin W.S., Chernoch J.P. U.S. Patent No. 3633126 (1972).
2. Rutherford T.S., Tulloch W.M., Sinha S., Byer R.L. *Opt. Lett.*, **26**, 986 (2001).
3. Goodno G.D., Palese S., Harkenrider J., Injeyan H. *Opt. Lett.*, **26**, 1672 (2001).
4. Gong M., Li C., Liu Q., Chen G., Gong W., Yan P. *Appl. Phys. B: Lasers and Optics*, **79**, 265 (2004).
5. Liu Qiang, Gong Mali, Li Chen, Wupeng Gong, Fuyuan Lu, Chen Gang. *Acta Phys. Sinica*, **54**, 721 (2005).
6. Liu Qiang, Gong Mali, Lu Fuyuan, Gong Wupeng, Li Chen. *Opt. Lett.*, **30**, 726 (2005).
7. Gong Mali, Lu Fuyuan, Liu Qiang, Gong Wupeng, Li Chen. *Appl. Opt.*, **45**, 3806 (2006).
8. Liu Qiang, Gong Mali, Lu Fuyuan, Gong Wupeng, Li Chen, Ma Dongdong. *Appl. Phys. Lett.*, **88**, 101113 (2006).
9. Kaminskii A.A. *Laser Crystals: Their Physics and Properties* (New York: Springer-Verlag, 1990).